Piezoelectric response of porous ceramic and composite materials based on $Pb(Zr,Ti)O_3$: experiment and modelling

V. Yu. Topolov[1], S. V. Glushanin[1] and C. R. Bowen*[2]

The present paper presents experimental and theoretical studies of the effective piezoelectric properties of porous $Pb(Zr,Ti)O_3$ based ceramics and composites. The experimental dependence of piezoelectric coefficients and dielectric permittivity on relative density is determined for porous materials containing different piezopassive components. The piezoelectric response of these materials in a wide range of volume concentrations of the piezopassive components are analysed in the framework of a model of a modified laminated composite with 2–2 and 1–3 connectivity elements. The role of these elements in forming different concentration dependences of the effective parameters of the porous piezoceramic and piezocomposite materials is discussed.

Keywords: Composites, Modelling, Piezoelectricity, Porosity

Introduction

Ferroelectric perovskite type ceramics and composites are modern functional heterogeneous materials characterised by a wide spectrum of piezoelectric, dielectric, pyroelectric and other properties. These materials have been developed, for example, to meet requirements for high effectiveness and efficiency of piezoactive elements for electromechanical transducer, hydrophone and piezotechnical applications. Many experimental studies point out that the effective physical properties of piezoactive ceramics and composites depend essentially on microstructure and the volume concentrations of the components. In this sense, a material containing a piezoactive component distributed through its bulk in a variety of configurations is of particular interest. Porous ceramics and composites based on ferroelectric $Pb(Zr,Ti)O_3$ perovskite type solid solutions are important examples of such piezoactive materials that have been intensively studied in the last decades and are potential materials for various hydrophone and piezotechnical applications.[1–8] Porous ceramics and composites offer considerable improvements over monolithic ceramics owing to large values of effective parameters such as hydrostatic piezoelectric coefficients $d_h^* = d_{33}^* + 2d_{31}^*$ and $g_h^* = g_{33}^* + 2g_{31}^*$,[2,6] piezoelectric coefficients d_{33}^* and g_{33}^*,[1,5–8] electromechanical coupling factors k_{33}^* and k_t^*,[3–5] and squared figures of merit $(Q_{33}^*)^2 = d_{33}^* g_{33}^*$ and $(Q_h^*)^2 = d_h^* g_h^*$.[7,8]

To the best of the present authors' knowledge, microstructural studies of porous piezoactive ceramic and composite materials have been carried out by only a few workers.[1,4,6,8] Many processing routes result in microstructures containing mixtures of isolated and interconnected pores described by 3–0 or 3–3 connectivity,[1–8] respectively, in the terminology of Newnham *et al.*[9] For analysis of the effective piezoelectric, dielectric, elastic and other properties of these materials, different micromechanical models have been put forward.[3,4,8,10–12] However, apart from the procedure described in Ref. 13, the existing theoretical approaches do not enable modelling of the microstructure–property relationships for both 3–0 and 3–3 connectivities. This approach stimulates a search for new methodologies for characterisation of microstructures and for microstructural elements influencing physical properties. The present paper reports experimental data on porous $Pb(Zr,Ti)O_3$ based ceramics and composites and attempts to describe features of the piezoelectric response of these materials in the framework of a model of a modified laminated composite with 2–2 and 1–3 connectivity elements.[14]

Properties of porous materials

Experimental results

Figures 1–5 present typical properties of porous piezoelectric materials (PZT–air) including polymer impregnated ceramic foams (PZT–polymer). Precise processing details and measurement methods are presented elsewhere.[15,16] Low density piezoelectric foams (<0·3 relative density) were prepared by coating polymeric foams with a ceramic suspension and sintering. The higher density materials (>0·3 relative density) were fabricated using a variety of volatile additives added to the ceramic powder before uniaxial pressing. The additives include polymethylmethacrylate (PMMA), polyethylene oxide (PEO), self-raising flour (SR) and corn starch (CS), which all produce porosity within the

[1]Department of Physics, Rostov State University, ul. Zorge 5, 344090 Rostov-on-Don, Russia
[2]Materials Research Centre, Department of Mechanical Engineering, University of Bath, Bath BA2 7AY, UK

*Corresponding author, email C R Bowen [msscrb@bath.ac.uk]

Published by Maney on behalf of the Institute
Received 9 May 2005; accepted 8 August 2005
DOI 10.1179/174367605X73335

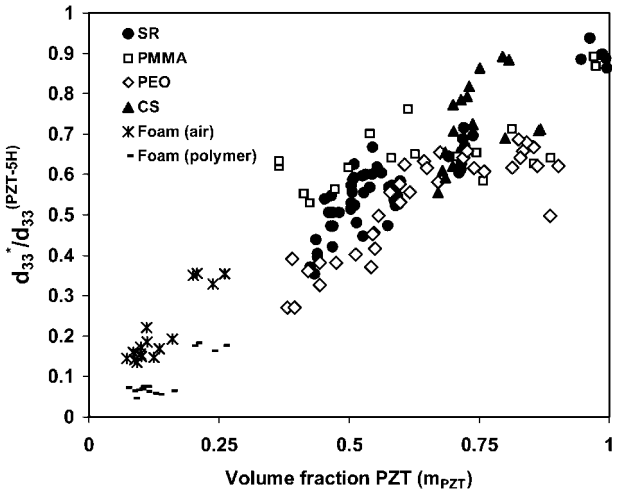

1 Variation of $d_{33}^*/d_{33}^{(PZT-5H)}$ with PZT fraction for all samples: SR=self-raising flour, PMMA=polymethylmethacrylate, PEO=polyethylene oxide, CS=corn starch

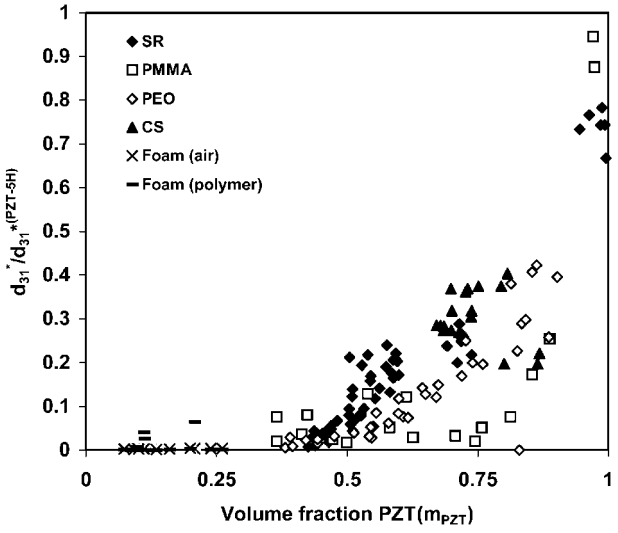

2 Variation of $d_{31}^*/d_{31}^{(PZT-5H)}$ with PZT fraction

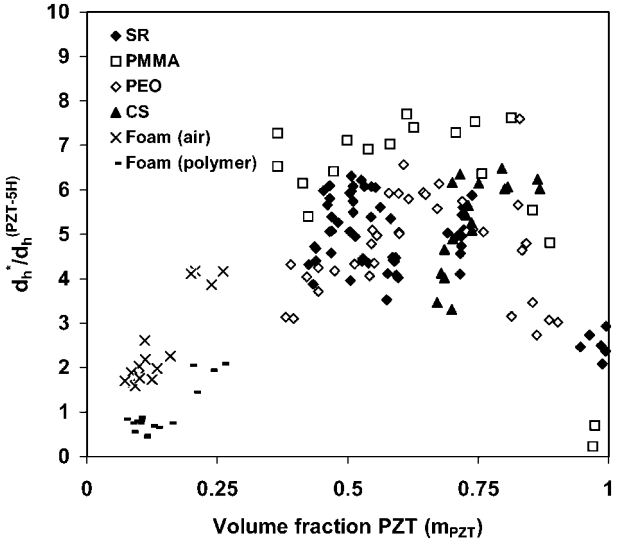

3 Variation of $d_h^*/d_h^{(PZT-5H)}$ with PZT fraction

ceramics on volatilisation during heat treatment. In all cases PZT-5H was used as the ceramic component and all results are normalised with respect to the properties

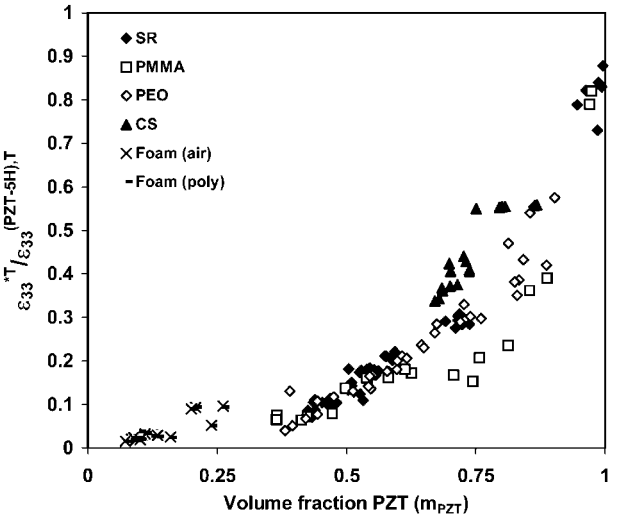

4 Variation of $\varepsilon_{33}^{*T}/\varepsilon_{33}^{(PZT-5H),T}$ with PZT fraction

of the dense material. The scatter in the data in Figs. 1–5 is thought to originate from the different microstructures formed by the different inclusion types and sizes. For example, PMMA based materials exhibit cracking parallel to the pressing (and poling) direction, leading to low effective permittivity.[15]

Figure 1 shows d_{33}^* against volume fraction of PZT m_{PZT} for foams and porous materials manufactured from the different inclusion materials. The general trend is a decrease in the value of d_{33}^* with decreasing m_{PZT}. This trend shows a distinct dependence of d_{33}^* on porosity volume concentration at low values of m_{PZT} ($<0{\cdot}75$) and lower dependence at high m_{PZT} ($>0{\cdot}75$). It can also be seen that different production methods produce different d_{33}^* values for the same relative density.

Variations amongst additives are related to the different connectivities of the porous structures formed within the material. The variation of d_{31}^* with m_{PZT} is shown in Fig. 2. Again the general trend is that the absolute value of d_{31}^* decreases with decreasing relative density, but at a more rapid rate than d_{33}^* (particularly in the high density range). Such a decrease in d_{31}^* suggests that an electromechanical interaction between some piezoactive elements aligned in the poling direction becomes weaker as the porosity of the material surrounding these elements increases. The rapid

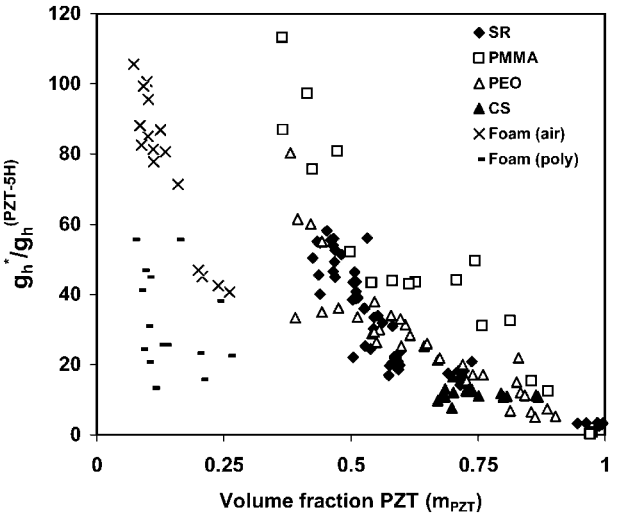

5 Variation of $g_h^*/g_h^{(PZT-5H)}$ with PZT fraction

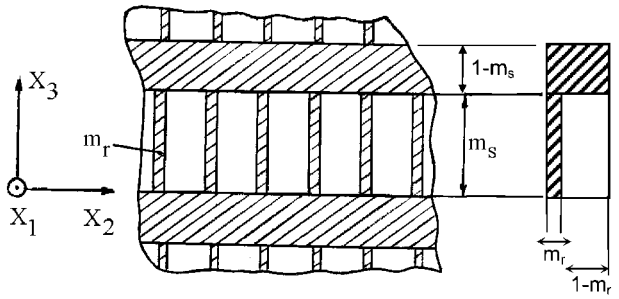

6 Schematic diagram showing structure of porous piezoelectric ceramic or porous composite on basis of piezoelectric ceramic: dashed area is monolithic ceramic component characterised by remanent polarisation vector $P_R \uparrow \uparrow OX_3$; clear area is passive phase (air, polymer or porous polymer)

decrease in d_{31}* and subsequent increase in piezoelectric anisotropy (d_{33}*/d_{31}*) results in high effective d_h* values, as observed in Fig. 3. A maximum of d_h* is present at m_{PZT} of 0·5–0·75. The highest values of d_h* are obtained using PMMA as the inclusion material. The foam based materials, while having a modest value of d_h* (100–200 pC N^{-1}), still show a higher value than for dense PZT-5H (around 50 pC N^{-1}). These foam materials have many other material property advantages in their favour, including low density and acoustic impedance.

Figure 4 plots normalised relative permittivity against PZT volume fraction m_{PZT}. The results for samples made with PEO and SR have similar values as a function of density. The samples made with PMMA however have lower values of permittivity than expected, owing to cracking present in these samples perpendicular to the poling direction.[15] The CS samples have a higher permittivity, possibly due to its small pores, and a large amount of the bulk material is left continuous. The g_h* (d_h*/$\varepsilon_{33}{}^T$) data are presented in Fig. 5, where a high value of g_h results in a high electric field per unit hydrostatic stress and is a particularly important merit index for hydrophone applications. PMMA samples have high values of g_h arising from their suppressed values of ε_{33}* and d_{31}* caused by cracking of samples during manufacture. It can also be seen that the CS samples have a lower value of g_h* than the PEO and SR samples, owing to the high permittivity values of the CS samples. PZT–air foam based materials exhibit high g_h* but are difficult to use owing to their poor mechanical strength, however the PZT–polymer foam based materials, while having a lower value of g_h, are more robust and still well suited to applications such as hydrophones.

Model results

The considerable increase in piezoelectric anisotropy d_{33}*/d_{31}* and distinct decrease in d_{31}* on increasing the porosity or volume concentration of the piezopassive components m_p (polymer, porous polymer or air) are possibly a result of the presence of elements of the structure with 2–2 connectivity, i.e. layers of piezoceramic. An example of the structure of a modified laminated composite has been considered elsewhere.[13] Based on these results, a model containing two types of piezoactive layers is put forward, as shown in Fig. 6. The remanent polarisation vectors $\boldsymbol{P}_{R,i}$ are assumed to be oriented perpendicular to interfaces. The slight decrease in d_{33}* with increasing m_p results from a continuous distribution of the piezoceramic framework along the poling axis OX_3, and it can take place with the presence of elements in the structure with 1–3 connectivity. According to this model, the layer of the first type represents a passive matrix reinforced by a system of piezoceramic cylindrical rods being lengthy and parallel to the poling axis OX_3. The layer of the second type is assumed to be piezoceramic and lengthy in both OX_1 and OX_2 directions. These layers, which alternate along the OX_3 direction, are the main elements of the structure of porous ceramic or composite materials and the volume concentrations of their piezoactive (m_{PZT}) and piezopassive (m_p) components can be determined from Fig. 6. If m_r and 1–m_r are respectively volume concentrations of the piezoceramic rods and the surrounding passive matrix (polymer, porous polymer or air), and m_s is the volume concentration of the layers containing the abovementioned piezoceramic rods, then $m_{PZT}=m_s m_r+1-m_s$ and $m_p=m_s(1-m_r)$. An additional effect of porosity can be taken into account if the polymer matrix is considered as a cellular structure with uniformly distributed spherical air inclusions, and the volume concentration of these air inclusions is m_{in}.

The effective parameters $x^*=e_{3j}$*, d_{3j}*, $\varepsilon_{33}{}^S$* and $\varepsilon_{33}{}^T$* (e_{3j}* are piezoelectric coefficients and $\varepsilon_{33}{}^S$* is dielectric permittivity measured at constant strain) of the porous material poled along the OX_3 axis are calculated using formulas for two component piezoactive composites in three stages. Averaging on m_{in} is carried out on the basis of formulas in Ref. 12 (0–3 connectivity), averaging on m_r follows formulas in Ref. 17 (1–3 connectivity) and averaging on m_s is enabled using formulas in Ref. 18 (2–2 connectivity). Calculations used room temperature experimental electromechanical constants of the following components: poled ferroelectric ceramic PZT-5H,[11] polyethylene[13] and elastomer.[17] Some examples of concentration behaviour of normalised effective parameters of porous PZT-5H based materials are shown in Table 1, where the superscript (PZT-5H) denotes the dense ceramic. Figure 7 presents modelled values of d^*_{33}, d^*_{31}, d^*_h, $\varepsilon_{33}{}^T$*, g^*_h as a function of PZT fraction, where the axes are to the same scale as the experimental data in Figs. 1–5 for direct comparison.

The calculated parameters can be compared in two ways. First, the comparison of effective parameters x* or ratios $x^*/x^{(PZT\text{-}5H)}$ in cases I and II in Table 1 permits the conclusion that the substitution of polyethylene by a more compliant polymer (an elastomer) results in a slight increase in dielectric permittivity $\varepsilon_{33}{}^T$*(m_s,m_r) and d_{3j}*(m_s,m_r), but a more significant increase in piezoelectric coefficients d_{3j}*(m_s,m_r), d_h*(m_s,m_r) and g_h*(m_s,m_r) at fixed concentration parameters m_s and m_r. This substitution influences the piezoelectric anisotropy d_{33}*(m_s,m_r)/d_{31}*(m_s,m_r), mainly as a result of the change in the ratio $c_{11}{}^{(p)}/c_{12}{}^{(p)}$ of the polymer elastic moduli. Second, comparing data from cases II, III and IV in Fig. 7, it can be concluded that the changes in $\varepsilon_{33}{}^T$*(m_s,m_r) and d_{31}*(m_s,m_r) are not considerable. However, values of d_{33}*(m_s,m_r), d_h*(m_s,m_r) and g_h*(m_s,m_r) increase when the elastomer matrix is substituted by a more compliant porous elastomer or by air. It is proposed that such behaviour is accounted for by the weak electromechanical interaction between piezoceramic rods in the OX_1 and OX_2 directions, owing

to the presence of the piezopassive matrix, and for conditions favourable to the 'rod–layer' electromechanical interaction in the OX_3 direction. As is known from earlier work,[17,19] in 1–3 piezoactive composites, softening the matrix surrounding the piezoelectric rods provides higher values of effective piezoelectric coefficients d_{33}*, g_{33}*, d_h* and g_h*, even at small volume concentrations of the rods. In addition, an important consequence of the slight concentration dependence of d_{33}*(m_s,m_r) in cases II and III (Table 1) is the equality g_{33}*/$g_{33}^{(PZT\text{-}5H)}$=(Q_{33}*)^2/($Q_{33}^{(PZt\text{-}5H)}$)^2, which holds true with accuracy up to a few per cent.

The correlation between experimental (Figs. 1–5) and calculated (Fig. 7) concentration dependences exists in a wide m_p range with changing m_s and m_r parameters of layers of the first type (Fig. 6). As m_p increases, the concentration parameter m_s also increases, and the relation $m'_p/m_p \approx m'_s/m_s$ remains correct at $0{\cdot}10 < m_p < 0{\cdot}60$, where m'_s is the concentration parameter analogous to m_s, but at porosity $m'_p \neq m_p$. As m_p approaches 0·60, a comparison of experimental and calculated parameters becomes problematic. These parameters would be in good agreement at $m_r < 0{\cdot}10$, however the structure of the porous composite with

Table 1 Calculated ratios of parameters $x^*/x^{(PZT\text{-}5H)}$ of composite materials based on PZT-5H: $m_p = m_s(1-m_r)$, $m_{PZT} = m_s m_r + 1 - m_s$, $m_p + m_{PZT} = 1$; in case III, volume concentration of spherical air pores in elastomer matrix is $m_{in} = 0{\cdot}30$

m_s	m_r	$m_p(=1-m_{PZT})$	$\varepsilon_{33}^{*T}/\varepsilon_{33}^{(PZT\text{-}5H),T}$	$d_{31}^*/d_{31}^{(PZT\text{-}5H)}$	$d_{33}^*/d_{33}^{(PZT\text{-}5H))}$	$d_h^*/d_h^{(PZT\text{-}5H)}$	$g_h^*/g_h^{(PZT\text{-}5H)}$
Case I: PZT-5H–polyethylene							
0·10	0·08	0·092	0·398	0·413	0·724	2·68	6·76
0·15	0·10	0·135	0·368	0·388	0·745	3·00	8·16
0·20	0·10	0·180	0·304	0·327	0·720	3·20	10·5
0·25	0·13	0·218	0·329	0·355	0·771	3·40	10·3
0·30	0·12	0·264	0·269	0·299	0·738	3·51	13·0
0·35	0·12	0·308	0·240	0·273	0·728	3·60	15·0
0·40	0·10	0·360	0·180	0·215	0·672	3·56	19·8
0·45	0·10	0·405	0·163	0·202	0·667	3·60	22·1
0·50	0·09	0·455	0·133	0·175	0·634	3·53	26·5
0·55	0·06	0·517	0·0779	0·117	0·519	3·43	39·2
0·60	0·05	0·570	0·0584	0·0984	0·468	2·80	48·0
0·65	0·04	0·624	0·0419	0·0821	0·409	2·47	59·1
Case II: PZT-5H–elastomer							
0·10	0·08	0·092	0·437	0·445	0·872	3·61	8·26
0·15	0·10	0·135	0·402	0·412	0·885	3·93	9·77
0·20	0·10	0·180	0·335	0·346	0·872	4·26	12·7
0·25	0·13	0·218	0·356	0·368	0·900	4·32	12·2
0·30	0·12	0·264	0·295	0·308	0·883	4·58	15·6
0·35	0·12	0·308	0·264	0·279	0·878	4·74	18·0
0·40	0·10	0·360	0·201	0·218	0·847	4·91	24·4
0·45	0·10	0·405	0·183	0·201	0·843	4·99	27·3
0·50	0·09	0·455	0·151	0·171	0·823	5·05	33·4
0·55	0·06	0·517	0·0917	0·112	0·744	4·85	52·9
0·60	0·05	0·570	0·0697	0·0913	0·703	4·69	67·2
0·65	0·04	0·624	0·0508	0·0737	0·650	4·42	86·9
Case III: PZT-5H–porous elastomer							
0·10	0·08	0·092	0·459	0·460	0·962	4·13	9·00
0·15	0·10	0·135	0·420	0·422	0·967	4·40	10·5
0·20	0·10	0·180	0·352	0·354	0·963	4·80	13·6
0·25	0·13	0·218	0·370	0·373	0·972	4·75	12·8
0·30	0·12	0·264	0·309	0·311	0·966	5·10	16·5
0·35	0·12	0·308	0·277	0·280	0·965	5·29	19·1
0·40	0·10	0·360	0·214	0·217	0·955	5·61	26·2
0·45	0·10	0·405	0·195	0·199	0·954	5·72	29·4
0·50	0·09	0·455	0·162	0·166	0·947	5·87	36·3
0·55	0·06	0·517	0·101	0·106	0·917	6·04	59·8
0·60	0·05	0·570	0·0778	0·0833	0·900	6·06	77·8
0·65	0·04	0·624	0·0577	0·0638	0·876	6·00	104
Case IV: PZT-5H–air							
0·10	0·08	0·092	0·466	0·466	1	4·37	9·38
0·15	0·10	0·135	0·426	0·426	1	4·62	10·8
0·20	0·10	0·180	0·358	0·358	1	5·05	14·1
0·25	0·13	0·218	0·375	0·375	1	4·95	13·2
0·30	0·12	0·264	0·313	0·313	1	5·34	17·0
0·35	0·12	0·308	0·281	0·281	1	5·54	19·7
0·40	0·10	0·360	0·218	0·218	1	5·94	27·2
0·45	0·10	0·405	0·198	0·199	1	6·06	30·5
0·50	0·09	0·455	0·166	0·166	1	6·27	37·8
0·55	0·06	0·517	0·104	0·104	1	6·65	63·7
0·60	0·05	0·570	0·0811	0·0811	1	6·80	83·9
0·65	0·04	0·624	0·0607	0·0607	1	6·93	114

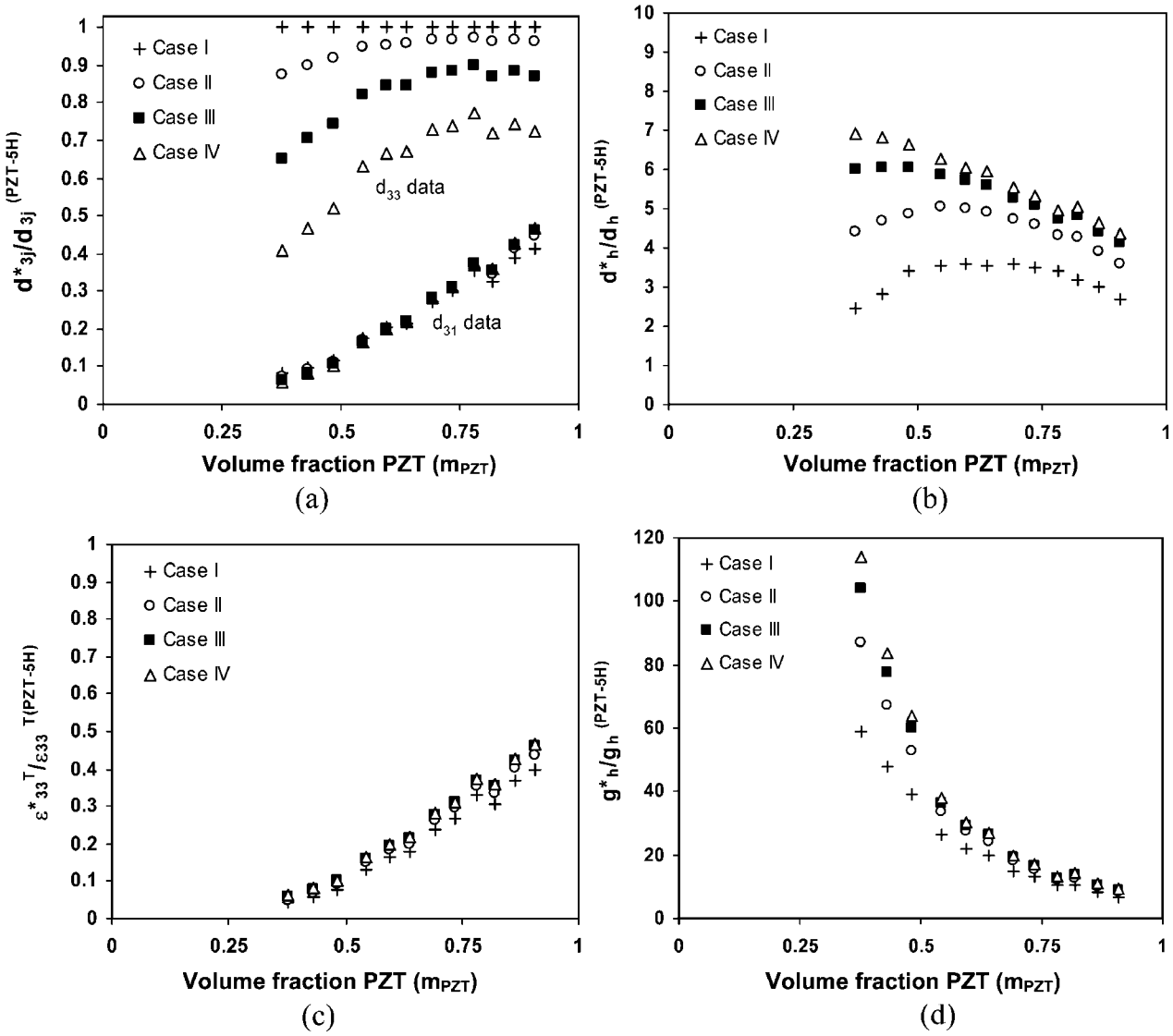

7 Model outputs of composite: *a* d^*_{33} (upper data), d^*_{31} (lower data); *b* d^*_h; *c* $\varepsilon_{33}{}^{*T}$; *d* g^*_h. All values normalised with respect to dense material (where $d_{33}=593$ pC N^{-1}, $d_{31}=-274$ pC N^{-1}, $\varepsilon_{33}{}^{T}=3400$)

small m_r values at $m_s>2/3$ becomes unstable and may be destroyed by a small amount of mechanical loading. Apparently this fact emphasises the upper bound of volume concentration such that $m_p<0{\cdot}60$ and $m_{PZT}>0{\cdot}4$ is the most suitable range where the proposed model can be used for interpretation of experimental data.

Conclusions

The effective piezoelectric and dielectric properties of porous $Pb(Zr,Ti)O_3$ based ceramics and composites have been analysed for a variety of piezotechnical applications. Based on the experimental data related to these piezoactive materials, a new model of the porous composite (ceramic) has been proposed to describe the experimental dependence of the effective parameters on porosity and other factors. Within the framework of this model, the composite sample is considered to be divided into structural elements with 1–3 (rods) and 2–2 (layers) connectivity. These elements play an important role in forming the dielectric and piezoelectric response and the variable piezoelectric anisotropy of the porous media in the wide porosity and polymer range. It is seen that both piezoelectric sensitivity and anisotropy of the porous ceramics and composites are closely predicted in terms of the concentration parameters. Moreover, as follows from comparison of the experimental and calculated results, the upper bound $m_p=0{\cdot}60$ is a realistic estimate where the proposed model is reliable for microstructural design and optimisation of porous piezoactive materials for specific applications.

Acknowledgements

The authors are grateful to Prof. Dr A. V. Turik and Prof. Dr A. E. Panich (Rostov State University, Russia) for their continued interest in the research problems.

References

1. K. Hikita, K. Yamada, M. Nishioka and M. Ono: *Jpn. J. Appl. Phys.*, 1983, **22**, Suppl. 2, 64–66.
2. R. Ting: *Ferroelectrics*, 1985, **65**, 11–20.
3. W. Wersing, K. Lubitz and J. Mohaupt: *Ferroelectrics*, 1986, **68**, 77–97.
4. U. Bast and W. Wersing: *Ferroelectrics*, 1989, **94**, 229–242.
5. S. S. Lopatin and T. G. Lupeiko: *Neorg. Mater.*, 1991, **27**, 1948–1951 (in Russian).
6. M. J. Creedon and W. A. Schulze: *Ferroelectrics*, 1994, **153**, 333–339.
7. H. Kara, A. Perry, R. Stevens and C. R. Bowen: *Ferroelectrics*, 2002, **265**, 317–322.

8. H. Kara, R. Ramesh, R. Stevens and C. R. Bowen: *IEEE Trans. Ultrason., Ferroelec., Freq. Control*, 2003, **50**, 289–296.
9. R. E. Newnham, D. P. Skinner and L. E. Cross: *Mater. Res. Bull.*, 1978, **13**, 525–536.
10. H. Banno: *Jpn. J. Appl. Phys.*, 1985, **24**, Suppl. 2, 445–447.
11. M. Dunn and M. Taya: *J. Am. Ceram. Soc.*, 1993, **76**, 1697–1706.
12. M. Dunn: *J. Appl. Phys.*, 1995, **78**, 1533–1541.
13. F. Levassort, M. Lethiecq, P. Desmare and L. P. Tran-Huu-Hue: *IEEE Trans. Ultrason., Ferroelec., Freq. Control*, 1999, **46**, 1028–1034.
14. V. Yu. Topolov and A. V. Turik: *Tech. Phys. Lett. (Russia)*, 1988, **24**, 441–443.
15. C. R. Bowen, A. Perry, A. C. F. Lewis and H. Kara: *J. Eur. Ceram. Soc.*, 2004, **24**, 541–545.
16. R. Ramesh, H. Kara and C. R. Bowen: *Ferroelectrics*, 2002, **273**, 2761–2766.
17. A. A. Grekov, S. O. Kramarov and A. A. Kuprienko: *Mech. Compos. Mater. (USSR)*, 1989, **25**, (1), 54–61.
18. L. P. Khoroshun, B. P. Maslov and P. V. Leshchenko: 'Prediction of effective properties of piezoactive composite materials'; 1989, Kiev, Naukova Dumka (in Russian).
19. V. Yu. Topolov and A. V. Turik: *J. Appl. Phys.*, 1999, **85**, 372–379.